Equivalent Parameters of Metal-Elastomer Vibroinsulators

Grzegorz CIEPLOK, Kaja WÓJCIK, Krzysztof MICHALCZYK, Wojciech SIKORA
AGH University of Science and Technology,
al. Mickiewicza 30, Krakow,
cieplok@agh.edu.pl, kwojcik@agh.edu.pl
kmichal@agh.edu.pl, wsikora@agh.edu.pl

Abstract

This paper concerns a substitute model of the metal-elastomer vibroinsulator that can find use in the mathematical description of vibration machine suspensions. In the case of a plane system, the flexibility matrix of the vibroinsulator was derived and two typical configurations of machine suspensions: symmetrical and asymmetrical, were analysed. For the case of a spatial motion, the elastic matrix of the vibroinsulator and the method of determining its elements was specified. Due to the non-linear character of the vibroinsulator's work, which is caused by large deformations of elastomeric elements under static loads, the analysis was limited to the surroundings of the work point and linear model. The results of theoretical analyses were confirmed by experimental tests.

Keywords: metal-elastomer vibroinsulators, vibratory machines, general motion

1. Introduction

Due to the character of their work, vibratory machines are based on elastic elements. This type of elements can include e.g.: helical springs, parallel leaf-springs, rubber connectors or metal-elastomer vibroinsulators. The last ones, are different from the others, due to their more complicated construction and operation character [1,2]. Strong couplings between the directions of the movement, make it impossible to easily discern fixed axes of operation, as for example in the case of helical springs. Such an element, even under an influence of a constant force, deforms in a complex way by taking a spatial shape. The proper mathematical description of the vibroinsulators is fundamental for a proper description of the machine operation, mainly due to the natural frequencies of the machine - suspension system. They perform a key role in the synchronization process of the inertial vibrators [3,4], as well as in the transition states associated with the start-up and run-down of the machine [5,6,7]. The energy loss in the element during its long term continuous running is also significant.

This paper takes on the task of formulating such model. The basic criterion for the model was to represent the properties of the element in the form of a discrete model that includes the elasticity of the element. The model should be simple enough to provide an engineering method to determine its physical parameters. The elastomer, which is the active part of a vibroinsulator, is generally subjected to two kinds of deformation: a strong one, caused by a static load of the machine and a small one, related to the machine vibrations. The first, may introduce elastomer into the non-linear work, while the second causes the virtually linear work.

In this paper the linear model of the vibroinsulator, which is limiting itself to working around the static deflection point of the element, was adopted. This is a widely used approach, related to the linearization of non-linear force-displacement characteristics of the element in the work point area. The force-displacement characteristics may be determined using the finite element method implementing hyperelastic materials. After determining the appropriate gradients, it is possible to determine the elasticity matrix. This matrix describes the vibroinsulator by 36 coefficients and allows to model its operation in a spatial motion. With an engineering drawing of the vibroinsulator (usually provided by the manufacturers), and an elastomer model (linear, nonlinear) the process of determining the matrix coefficients can be algorithmized.

A very important issue is a system in which vibroinsulators work. The parameters of the elastic matrix of a single vibroinsulator do not easily convert into the parameters of the elastic matrix of the suspension system. Therefore, in the first part of the paper the analysis of two typical configurations of metal-elastomeric vibration insulators - used in vibration machine suspensions - was performed.

The results of the theoretical analyses were compared with the results of laboratory measurements and with the parameters presented in the manufacturer's catalogue.

2. Model of the metal-elastomer vibroinsulator in a plane system

A typical metal-elastomer vibroinsulator is shown in Fig. 1. It consists of metal arms and fixing elements, connected with each other by elastomeric inserts. The construction of the vibroinsulator in the form of an oscillating pantograph allows for a high deflection under load. It causes a low natural vibration frequencies of the vibro-insulated mass and therefore a high vibration efficiency. In turn, the great lateral stability of the vibroinsulators prevents lateral fluctuations of the vibro-insulated mass that occur e.g. during passing through resonance frequencies (so characteristic of helical springs [8]). Fig. 2 shows the model of the vibroinsulator corresponding to Fig. 1. It consists of four arms connected by joints exposed to angular springs which represent elastomeric inserts. The upper arm, with which the vibroinsulator is attached to the body of the machine, is loaded with force and the moment of force.

For the system formulated in this way, the equilibrium conditions between the extortion and the angular movements of the vibroinsulator arms can be presented in the form of a relation (1.a-d).

Figure 1. Photography of the vibroinsulator

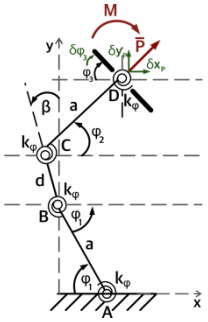

Figure 2. Model of the vibroinsolator

$$k_\varphi(2\cdot\delta\varphi_1+\beta)=a\cdot(P_x\cdot\sin\varphi_1+P_y\cdot\cos\varphi_1) \quad (1.a)$$

$$k_\varphi(\delta\varphi_1+2\cdot\beta-\delta\varphi_2)=-d\cdot(P_x\cdot\cos\beta+P_y\cdot\sin\beta) \quad (1.b)$$

$$k_\varphi(2\cdot\delta\varphi_2-\beta+\delta\varphi_3)=a\cdot(P_y\cdot\cos\varphi_2-P_x\cdot\sin\varphi_2) \quad (1.c)$$

$$k_\varphi(\delta\varphi_3+\delta\varphi_2)=M \quad (1.d)$$

These relations lead to:

$$\begin{bmatrix}\delta x_p\\ \delta y_p\\ \delta\varphi_3\end{bmatrix}=\begin{bmatrix}d_{11} & d_{12} & d_{13}\\ d_{12} & d_{22} & d_{23}\\ d_{13} & d_{23} & d_{33}\end{bmatrix}\begin{bmatrix}P_x\\ P_y\\ M\end{bmatrix} \quad (2)$$

$$d_{11}=\frac{6a^2\sin(\varphi_2)^2+6ad\cos(\beta)\sin(\varphi_2)+2d^2\cos(\beta)^2}{k_\varphi} \quad (2.a)$$

$$d_{12}=-\frac{(2a^2\cos(\varphi_2)-3ad\sin(\beta))\sin(\varphi_2)+ad\cos(\beta)\cos(\varphi_2)-2d^2\cos(\beta)\sin(\beta)}{k_\varphi} \quad (2.b)$$

$$D_{13}=\frac{4a\sin(\varphi_2)+2d\cos(\varphi_2)}{k_\varphi} \quad (2.c)$$

$$d_{22}=\frac{2a^2\cos(\varphi_2)^2-2ad\sin(\beta)\cos(\varphi_2)+2d^2\sin(\beta)^2}{k_\varphi} \quad (2.d)$$

$$d_{23}=-\frac{2a\cos(\varphi_2)-2d\sin(\beta)}{k_\varphi} \quad (2.e)$$

$$d_{33}=\frac{4}{k_\varphi} \quad (2.f)$$

in which [D] represents the flexibility matrix of the vibration insulator. The inverse matrix

$$[K]=[D]^{-1} \quad (3)$$

shows the elastic matrix and it can be used to determine the potential energy of the vibroinsulator.

The main difficulty in the practical application of this model is the lack of knowledge of the angular coefficient k_φ. In general, the technical documentation provided by the producer includes the averaged values of linear elastic coefficients (for vertical and

horizontal direction) and the natural vibration frequency range of the vibro-insulated mass. Without proper relations, such values do not allow for a mutual conversion of coefficients. In addition, the matter is further complicated by the non-linear character of the elastic coefficients depending on the load value [9].

Figures 3 and 4 show the results of the compression process in the vertical axis of the ROSTA ABI 15 vibroinsulator. The vertical displacement of the upper mounting plane of the vibroinsulator was determined within a range from 0 to 0.048 m, which corresponded to the full range of its work. The courses of forces and moments of the vibroinsulator's impact with fixation have linear waveforms, and the characteristic of the force F_z corresponds to the almost linear characteristic of the vibroinsulator presented in the manufacturer's catalogue.

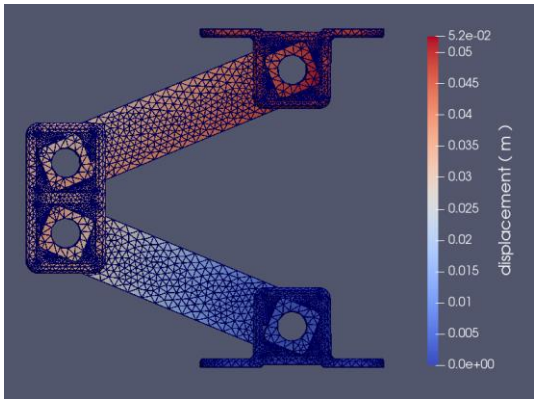

Figure 3. Model of the vibroinsulator in finite elements

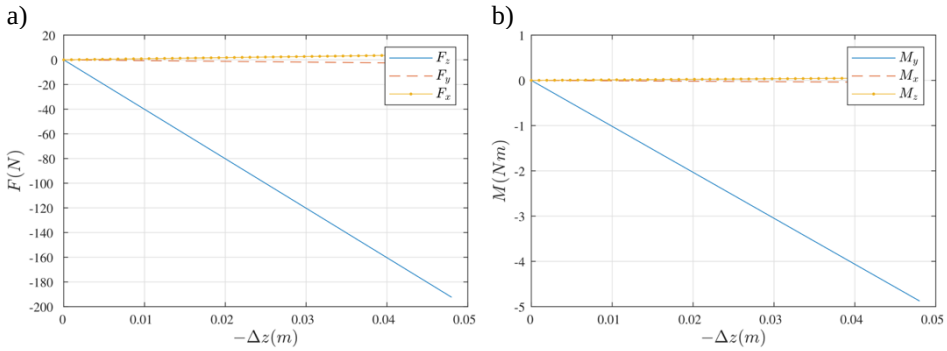

Figure 4. Dependence of reaction forces (a) and the moment of forces M (b) of the static deflection Δz

With the force-deflection characteristics the elastic matrix coefficients can be determined by calculating the derivatives related to their slope. The results of such an operation are: $k_{22} \cong 4.0\,{}^{\mathrm{kN}}/_{\mathrm{m}}$, $k_{12} \cong 0.09\,{}^{\mathrm{kN}}/_{\mathrm{m}}$, $k_{23} \cong -0.10\,{}^{\mathrm{kNm}}/_{\mathrm{m}}$.

Due to relation (3), the coefficients of the matrix of elasticity expressed in analytical form can be compared with those obtained from the numerical analysis. In this way, the coefficient k_{22} can be related to the angular elasticity coefficient k_φ by relation (4).

$$k_{22} = \frac{2a \sin\varphi_2 \,(a \sin\varphi_2 + d\cos\beta) + d^2 \cos\beta^2}{(2a^4 \cos{\varphi_2}^2 + a^2 d^2 \sin\beta^2)\sin{\varphi_2}^2 + a^2 d \cos{\varphi_2}^2 \cos\beta\,(2a\sin\varphi_2 + d\cos\beta)} \cdot k_\varphi \quad (4)$$

Based on dependence (4), the k_φ coefficient was determined for the ABI 15 vibroinsulator. It reached 0.37 Nm/°. This value allowed to identify the element which builds up the vibration insulator (15x40 'Rubmix 10') and to correct the k_φ value according to the static load.

The corrected value equivalent to 140 N load is set at 0.55 Nm/° and was used in the calculations in Chapter 3.

3. Suspensions of vibratory machines. Plane systems

Metal-elastomer vibroinsulators can be used in suspensions of vibratory machines in two ways: symmetrically (Fig. 5a) or asymmetrically (Fig. 5b). Due to the presence of mutual couplings, the systems are described by different equations. It should lead to a different behavior of the system. In order to check the differences between them, both systems were analyzed in more detail.

a) b)

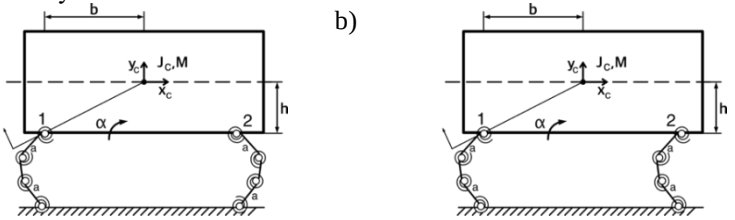

Figure 5. Symmetrical system (a). Asymmetrical system (b). x_C, y_C – coordinates of center of mass, α – rotation of the body

The potential energy accumulated in the vibroinsulator described by the matrix of elasticity [*K*] can be noted in the form of a relation:

$$V = \frac{1}{2}[\delta x_p \quad \delta y_p \quad \delta\varphi_3]\begin{bmatrix} k_{11} & k_{12} & k_{13} \\ k_{21} & k_{22} & k_{23} \\ k_{31} & k_{32} & k_{33} \end{bmatrix}\begin{bmatrix} \delta x_p \\ \delta y_p \\ \delta\varphi_3 \end{bmatrix} = \frac{1}{2}k_{11}{\delta x_p}^2 + \frac{1}{2}k_{22}{\delta y_p}^2 + \\ + \frac{1}{2}k_{33}{\delta\varphi_3}^2 + k_{12}\delta x_p \delta y_p + k_{13}\delta x_p \delta\varphi_3 + k_{23}\delta y_p \delta\varphi_3 \quad (5)$$

In the case of a symmetrical system, it will take the form:

$$V_{sym} = \frac{1}{2}k_{11}{x_1}^2 + \frac{1}{2}k_{22}{y_1}^2 + \frac{1}{2}k_{33}\alpha^2 + k_{12}x_1 y_1 + k_{13}x_1\alpha + k_{23}y_1\alpha + \\ + \frac{1}{2}k_{11}(-x_2)^2 + \frac{1}{2}k_{22}{y_2}^2 + \frac{1}{2}k_{33}(-\alpha)^2 + k_{12}(-x_2)y_2 + k_{13}(-x_2)(-\alpha) + \\ k_{23}y_2(-\alpha) \quad (6)$$

and in the case of an asymmetrical system, the form:

$$V_{asym} = \frac{1}{2}k_{11}{x_1}^2 + \frac{1}{2}k_{22}{y_1}^2 + \frac{1}{2}k_{33}\alpha^2 + k_{12}x_1y_1 + k_{13}x_1\alpha + k_{23}y_1\alpha + \\ + \frac{1}{2}k_{11}{x_2}^2 + \frac{1}{2}k_{22}{y_2}^2 + \frac{1}{2}k_{33}\alpha^2 + k_{12}x_2y_2 + k_{13}x_2\alpha + k_{23}y_2\alpha \quad (7)$$

where:

$$\delta x_1 = \delta x_c - h \cdot \delta\alpha \quad (8.a)$$
$$\delta y_1 = \delta y_c + b \cdot \delta\alpha \quad (8.b)$$
$$\delta x_2 = \delta x_c - h \cdot \delta\alpha \quad (8.c)$$
$$\delta y_2 = \delta y_c - b \cdot \delta\alpha \quad (8.d)$$

Based, for example, on the Lagrangian method of II kind, it is possible to determine dynamic motion equations for both cases [10]. On their basis, frequencies and forms of natural vibrations were determined. For parameters of the laboratory stand shown in Fig. 6: m = 59 kg, J_C = 6.26 kgm^2, b = 0.4 m, a = 0.08 m, d = 0.025 m, h = 0.15 m, the system's characteristic equation is as follows:

– for a symmetrical system:

$$-\begin{bmatrix} 59 & 0 & 0 \\ 0 & 59 & 0 \\ 0 & 0 & 6{,}26 \end{bmatrix}\omega^2 + \begin{bmatrix} 2{,}85 \cdot 10^4 & 0 & -5{,}57 \cdot 10^3 \\ 0 & 2{,}38 \cdot 10^4 & 0 \\ -5{,}57 \cdot 10^3 & 0 & 5{,}65 \cdot 10^3 \end{bmatrix} = 0 \quad (9)$$

– for asymmetrical system:

$$-\begin{bmatrix} 59 & 0 & 0 \\ 0 & 59 & 0 \\ 0 & 0 & 6{,}26 \end{bmatrix}\omega^2 + \begin{bmatrix} 2{,}85 \cdot 10^4 & 0 & -5{,}57 \cdot 10^3 \\ 0 & 2{,}38 \cdot 10^4 & 8{,}68 \cdot 10^2 \\ -5{,}57 \cdot 10^3 & 8{,}68 \cdot 10^2 & 4{,}96 \cdot 10^3 \end{bmatrix} = 0 \quad (10)$$

The natural frequencies (eigenvalues in Hz) and the corresponding eigenvectors [11] are respectively:

– for the symmetrical system:

$$\begin{bmatrix} 2.91 & 0 & 0 \\ 0 & 3.20 & 0 \\ 0 & 0 & 5.16 \end{bmatrix}\text{Hz} \qquad V_{sym} = \begin{bmatrix} -0.116 & 0 & -0.059 \\ 0 & 0.130 & 0 \\ -0.182 & 0 & 0.356 \end{bmatrix}$$

– for the asymmetrical system:

$$\begin{bmatrix} 2.77 & 0 & 0 \\ 0 & 3.21 & 0 \\ 0 & 0 & 4.95 \end{bmatrix}\text{Hz} \qquad V_{asym} = \begin{bmatrix} -0.108 & 0.030 & -0.067 \\ 0.030 & 0.126 & 0.009 \\ -0.205 & 0.025 & 0.342 \end{bmatrix}$$

As we can see, the differences between the natural frequencies, although they exist, are small and practically irrelevant. The comparison of the natural frequencies with the results of experimental measurements is similarly good. The following results were obtained for four measurement series:

– for the symmetrical system: $f_{0(horizontal)}$ =2.88 Hz and $f_{0(vertical)}$ = 3.15 Hz
– for the asymmetrical system: $f_{0(horizontal)}$= 2.98 Hz and $f_{0(vertical)}$ = 3.21 Hz

Figure 6. Photograph of the research stand. The suspension system based on AB 15 vibroinsulators

4. The potential energy of a spatial vibroinsulator

The potential energy of a spatial vibroinsulator in the work point can be expressed by a relation:

$$V = \frac{1}{2}\begin{bmatrix}\delta x_P\\ \delta y_P\\ \delta z_P\\ \delta\varphi_x\\ \delta\varphi_y\\ \delta\varphi_z\end{bmatrix}^T\begin{bmatrix}k_{11} & k_{12} & k_{13} & k_{14} & k_{15} & k_{16}\\ k_{12} & k_{22} & k_{23} & k_{24} & k_{25} & k_{26}\\ k_{13} & k_{23} & k_{33} & k_{34} & k_{35} & k_{36}\\ k_{14} & k_{24} & k_{34} & k_{44} & k_{45} & k_{46}\\ k_{15} & k_{25} & k_{35} & k_{45} & k_{55} & k_{56}\\ k_{16} & k_{26} & k_{36} & k_{46} & k_{56} & k_{66}\end{bmatrix}\cdot\begin{bmatrix}\delta x_P\\ \delta y_P\\ \delta z_P\\ \delta\varphi_x\\ \delta\varphi_y\\ \delta\varphi_z\end{bmatrix} \tag{11}$$

where: $\delta x_P, \delta y_P, \delta z_P, \delta\varphi_x, \delta\varphi_y, \delta\varphi_z$ describe the displacement coordinates of the unrestrained end (P) of the vibroinsolator, Fig. 7.

a) b)

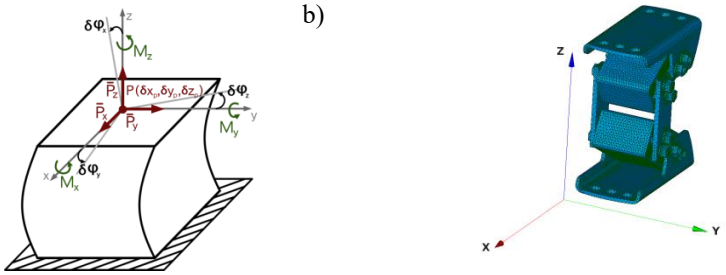

Figure 7. Model of a spatial spring. a) Coordinates and forces b) The orientation of the coordinate system used in the FEM analysis. In the figure, vibration isolator AB-D 18

Based on the methodology presented in Chapter 2, we determined selected coefficients of the elastic matrix of the AB-D 18 vibroinsulator. The value of the static deflection of the vibroinsulator was set at 16 mm, which is equivalent to one of the laboratory test loads.

On the basis of simple geometrical relations, the inclination angles of the vibroinsulator's arms $\varphi_1 = \varphi_2 = 26.7°$ and the corresponding rotation $\Delta\varphi = 18.3°$ were determined. On the basis of the catalogue characteristics $k_\varphi = f(\Delta\varphi)$, Table 1, the coefficient of angular elasticity of the element 18x50 forming the vibration insulator was determined. It amounted to 1.16 Nm/°.

Table 1. Catalogue data of ROSTA components [12]

Elament Nominal size x Length	Torque Md [Nm] angle $\pm\alpha°$						Cardanic Mk [Nm] angle $\pm\beta°$	Radial		Axial	
								Deflection $\pm s_r$	Load F_r	Deflection $\pm s_a$	Load F_a
	5°	10°	15°	20°	25°	30°	1°	[mm]	[N]	[mm]	[N]
18 x 30	1.9	4.5	7.5	11.0	15.0	20.6	1.6		400		80
50	3.2	7.5	12.5	18.3	25.0	43.4	7.0	0.25	700	0.25	160
80	5.1	12.0	20.0	29.3	40.0	55.0	28.0		1000		300

Based on the relation (4), for $a = 0.3$ m $b = 0.5$ m the value of

$$k_{33} = 86.6 \text{ kN/m} \tag{12}$$

(k_{22} in formula (4) corresponds to k_{33} in the elastic matrix. Such determined coefficient became the basis for the calibration of the Young's modulus in the FEM model. In this way, the modulus $E = 1.67$ MPa - corresponding to the elasticity of the elastomer at the point of its work - is determined. Fig. 8 shows the courses of forces and moments of forces during one-directional deformation of the vibroinsulator in Y direction, transverse to the proper working plane.

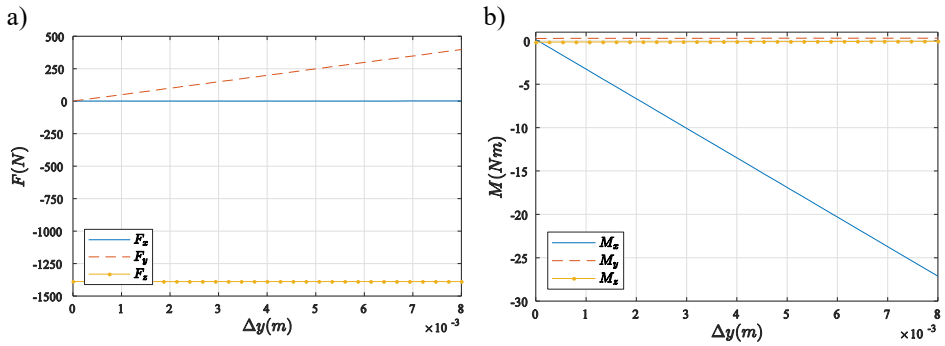

Figure 8. Courses of forces (a) and moments of forces (b) of the vibration insulator at the point of work, as a function of displacement Δy

Based on the characteristics slope angle, the following values were determined: k_{12} = 182 N/m, k_{22} = 49.7 kN/m, k_{23} = -173.5 kN/m, k_{24} = -3.4 kNm/m, k_{25} = 39.8 Nm/m, k_{26} = -5 Nm/m. The remaining coefficients can be determined analogically by assigning shifts to individual coordinates $\delta x_P, \delta z_P, \delta\varphi_x, \delta\varphi_y, \delta\varphi_z$.

In order to verify the correctness of the taken approach, experimental tests were carried out to confirm the value of the transverse elasticity coefficient k_{22}.

5. Experimental determination of the quasi-static lateral characteristics of AB-D 18 vibroinsulator

The test of the lateral stiffness of vibroinsulators was carried out on a test stand prepared for this purpose. The two tested vibroinsulators were placed in a frame made of Bosh-Rexroth strut profiles 45x45L, as shown in Fig. 9a. The tested vibroinsulators were connected in series with four screws. A steel plate was placed between the thrust surfaces. The overhanging part of the plate was then fixed in the holder of the HT-2402 testing machine (Fig. 9b). The external vibroinsulator bases were also attached to the frame with four screws. This system was fixed in the testing machine and by moving the holder, which holds the mounting plate, lateral oscillations of the vibroinsulators were forced. The lateral stiffness of the two vibroinsulators was thus measured under the conditions of double-sided clamping. Such attachment method reflects well the operating conditions of vibroinsulators where the machine vibrates in accordance with their working plane.

a) b)

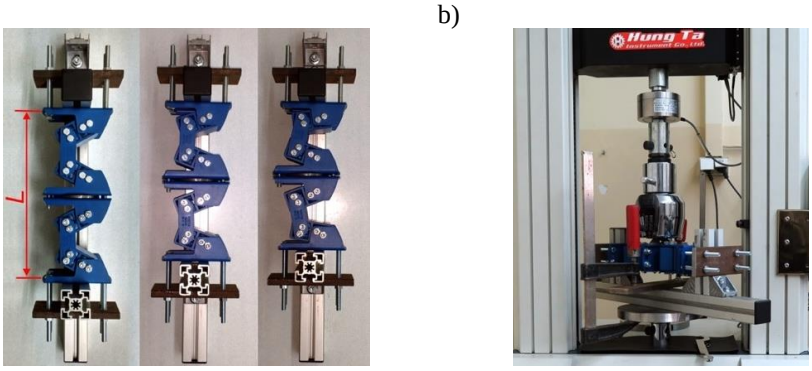

Figure 9. a) Tested system of two vibroinsulators at three different preloaded values. b) Test stand with attached tested system

During a single test, the machine's actuator, connected to the vibroinsulators system, performed 5 cycles of reciprocating motion with an amplitude of 8 mm. The speed of movement of the executive element was 25 mm/min and the sampling frequency was 0.1 s. The tests were performed for three different values of static deflection as shown in Fig. 10a. The L dimension determines the total height of the two vibroinsulators system including the mounting plate. The height of a single unloaded vibroinsulator was A = 137 mm. The tests were carried out for the following values of the total system height: L = 277 mm (preloaded shock absorbers: ΔA = 0), L = 261 mm (pre-bent absorbers, single shock absorber deflection is ΔA = 8 mm) and L = 245 mm (pre-bent absorbers, ΔA = 16 mm). The manufacturer states that the maximum pre-sagging value of a single vibroinsulator is 25 mm.

Fig. 10a shows examples of test results of vibroinsulators without a preload. We can see that the system response to extortion stabilizes relatively quickly and the results for all five cycles are very similar. The result of the tests also indicates small damping properties of the system at the tested rate of the actuator displacement.

In order to determine the quasi-static lateral stiffness of the vibroinsulators, tested under the conditions of bilateral restraint, the results of the fifth load cycle were used for each of the three pre-deflection values defined by dimension L. Fig. 10b presents the summary results of the lateral force-displacement courses obtained during the fifth load cycle for all three pre-deflection values.

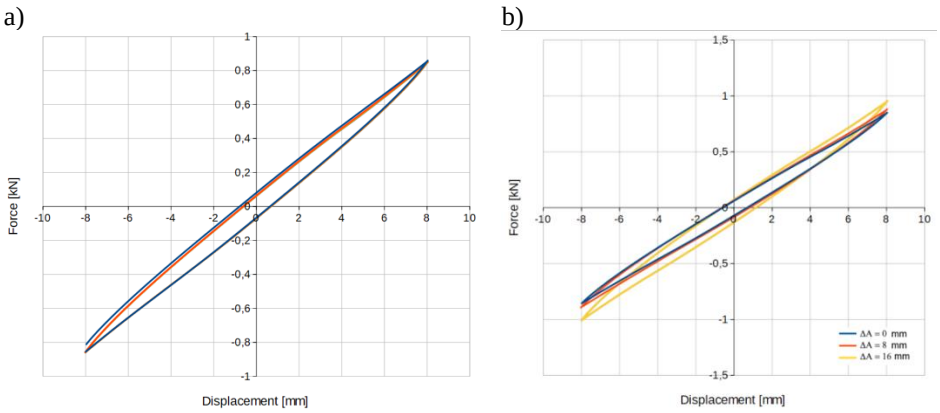

Figure 10. a) Response of tested system without preload
(L = 277 mm) to lateral force - recording all five load cycles
b) Summary of the fifth load cycle for all three values of ΔA

Based on the results presented in Fig. 10b, the linearized stiffness of a single vibroinsulator k_{22} and the energy dissipation coefficient Ψ, defined as the quotient of the energy dissipated for the entire load cycle to the maximum elastic energy, were determined. The obtained values are presented in Table 2.

Table 2. Lateral stiffness and the energy dissipation of vibroinsulators

	ΔA = 0	ΔA = 8 [mm]	ΔA = 16 mm
k_{22} [N/mm]	51.6	53.1	58.5
Ψ	0.4	0.45	0.56

Analyzing the results, it can be seen that with the increase of the static deflection of shock absorbers, their lateral stiffness as well as their energy dissipation coefficient are increasing.

6. Conclusions

The paper presents theoretical models and tests of metal-elastomer vibration insulators used in suspensions of vibratory machines. In the case of a vibroinsulator with the structure of a pantograph, operating in a plane system, the substitute model was proposed and on its basis the elements of the flexibility matrix were determined. The matrix became the starting point for determining the potential energy of the vibroinsulator. On these basis, it is possible to determine the forces of the interaction or include it in the case of construction complex systems in the Lagrange function. Two typical configurations of vibroinsulators used in machine suspensions were analyzed: symmetrical and asymmetrical, and differences between them were shown. There were presented the numerical analyses based

on the finite element method, on the basis of which the coefficients of elasticity matrix of the vibroinsulator can be directly determined and combined with the parameters of the substitute model. Experimental tests, based on the natural vibration frequencies of the machine, confirmed the high compatibility of theoretical calculations and experimental tests.

In the case of a spatial system, the potential energy of a vibration insulator is expressed by means of the 36-element elastic matrix. The matrix coefficients could be determined on the basis of force-displacement characteristics determined for a given static load. Due to the lack of material parameters in the technical documentation, necessary to perform numerical tests based on the finite element method, the authored method to determine the substitute Young's modulus of an elastomer, was developed. For this purpose, analytical relations derived for the model of the substitute vibroinsulator and angular elasticity characteristics of the part available in the manufacturer's catalogue were combined.

Experimental tests for verifying the theoretical model have confirmed its usefulness. For comparison of the transverse elasticity coefficient of a vibration insulator, the error below 16% was obtained $\left(\frac{58,5-49,7}{58,5}\right)$. Should be noted, that the deflection values shown in catalogue specifications should be understood as approximate values [12]. In order to obtain results with lesser errors, it is necessary to use an appropriate, testified material model with experimentally obtained material parameters.

The method presented in the paper allows, by means of an uncomplicated linear model of a vibroinsulator expressed in finite elements and calibrated on the basis of an angular elasticity parameter (provided by the manufacturer), to formulate the potential energy of the vibroinsulator as a function of motion coordinates, and therefore also to include the vibroinsulator in dynamic equations of movements of machines and equipment.

Acknowledgments

The work was carried out under the research subvention 16.16 130 942

References

1. S. Floody, J. Arenas, J. de Espindola, *Modelling metal-elastomer composite structures using a finite-element-method approach*, Journal of Mechanical Engineering, 53 (2) (2007) 66 – 77.
2. M. Ragni, D. Castagnetti, A. Spaggiari, F. Muccini, E. Dragoni, M. Milelli, S. Girlando, P. Borghi, *Shear Strength Characterization of Metal-Elastomer Bonded Joints*, FME Transactions, 45 (3) (2017) 360 – 366.
3. G. Cieplok, K. Wójcik*, Conditions for self-synchronization of inertial vibrators of vibratory conveyors in general motio*n, Journal of Theoretical and Applied Mechanics, 58 (2) (2020) 513 – 524.
4. J. Michalczyk, S. Pakuła, *Phase control of the transient resonance of the automatic ball balancer*, Mechanical Systems and Signal Processing (72-73) (2016) 254 –265.
5. G. Cieplok, *Verification of the nomogram for amplitude determination of resonance vibrations in the run-down phase of a vibratory machine*, Journal of Theoretical and Applied Mechanics, 47 (2) (2009) 295–306.

6. J. Michalczyk, Ł. Bednarski, *Overcoming of a resonance stall and the minimization of amplitudes in the transient resonance of a vibratory machine by the phase modulation method,* Journal of Engineering for Gas Turbines and Power, 132 (5) (2010) 052501-1 – 0502501-7.
7. P. Czubak, *Reduction of forces transmitted to the foundation by the conveyor or feeder operating on the basis of the Frahm's eliminator at a significant loading with feed*, Archives of Mining Sciences, 57 (4) (2012) 1121 – 1136.
8. K. Michalczyk, *Analysis of lateral vibrations of the axially loaded helical spring*, Journal of Theoretical and Applied Mechanics, 53 (3) (2015) 745 – 755.
9. W. Sikora, K. Michalczyk, T. Machniewicz, *Numerical modelling of metal-elastomer spring nonlinear response for low-rate deformations*, Acta Mechanica et Automatica, 12 (1) (2018) 31 – 37.
10. M. W. Dobry, *Energy Analysis of a Mechanical System with a Dynamic Vibration Absorber*, Vibrations in Physical Systems, 27 (2016) 83 – 90.
11. R. Lewandowski, *Approximate Method for Determination of Dynamic Characteristics of Structures with Viscoelastic Dampers*, Vibrations in Physical Systems, 27 (2016) 219 – 226.
12. *The Blue Ones from ROSTA Components for machine construction*, www.rosta.com**,** access from 06.06.2020.